

High-energy, ceramic-disk Yb:LuAG laser amplifier

M. Siebold,^{1,*} M. Loeser,¹ F. Roeser,¹ M. Seltmann,¹ G. Harzendorf,¹
I. Tsybin,¹ S. Linke,¹ S. Banerjee,² P.D. Mason,² P.J. Phillips,²
K. Ertel,² J.C. Collier,² and U. Schramm¹

¹*Helmholtz-Zentrum Dresden-Rossendorf, Bautzner Landstr. 400, 01328 Dresden, Germany*

²*Central Laser Facility, STFC Rutherford Appleton Laboratory, Didcot, OX11 0QX, UK*

[*m.siebold@hzdr.de](mailto:m.siebold@hzdr.de)

Abstract: We report the first short-pulse amplification results to several hundred millijoule energies in ceramic Yb:LuAG. We have demonstrated ns-pulse output from a diode-pumped Yb:LuAG amplifier at a maximum energy of 580 mJ and a peak optical-to-optical efficiency of 28% at 550 mJ. In cavity dumped operation of a nanosecond oscillator we obtained 1 mJ at up to 100 Hz repetition rate. A gain bandwidth of 5.4 nm was achieved at room temperature by measuring the small-signal single-pass gain. Furthermore, we compared our results with Yb:YAG within the same amplifier system.

© 2012 Optical Society of America

OCIS codes: (140.3280) Laser amplifiers; (140.3615) Lasers, ytterbium; (140.3480) Lasers, diode-pumped.

References and links

1. T. Metzger, A. Schwarz, C. Teisset, D. Sutter, A. Killi, R. Kienberger, and F. Krausz, "High-repetition-rate picosecond pump laser based on a Yb:YAG disk amplifier for optical parametric amplification," *Opt. Lett.* **34**, 2123–2125 (2009).
2. A. Giesen, and J. Speiser, "Fifteen years of work on thin-disk lasers: Results and scaling laws," *IEEE J. Quantum Electron. (ST)* **13**, 598–609 (2007).
3. D. Albach, J.-C. Chanteloup, and G. L. Touzé, "Influence of ASE on the gain distribution in large size, high gain Yb³⁺:YAG slabs," *Opt. Express* **17**, 3792–3801 (2009).
4. J. Mende, G. Spindler, J. Speiser, and A. Giesen, "Concept of neutral gain modules for power scaling of thin-disk lasers," *Appl. Phys. B* **97**, 307–315 (2009).
5. A. Curtis, B. Reagan, K. Wernsing, F. Furch, B. Luther, and J. Rocca, "Demonstration of a compact 100 Hz, 0.1 J, diode-pumped picosecond laser," *Opt. Lett.* **36**, 2164–2166 (2011).
6. K. Beil, S. Friedrich-Thornton, F. Tellkamp, R. Peters, C. Kränkel, K. Petermann, and G. Huber, "Thermal and laser properties of Yb:LuAG for kW thin disk lasers," *Opt. Express* **18**, 20712–20722 (2010).
7. A. Brenier, Y. Guyot, H. Canibano, G. Boulon, A. Ródenas, D. Jaque, A. Eganyan, and A. Petrosyan, "Growth, spectroscopic, and laser properties of Yb³⁺-doped Lu₃Al₅O₁₂ garnet crystal," *J. Opt. Soc. Am. B* **23**, 676–683 (2006).
8. D. Sumida, T. Fan, and R. Hutcheson, "Spectroscopy and diode-pumped lasing of Yb³⁺-doped Lu₃Al₅O₁₂ (Yb:LuAG)," *Advanced Solid State Lasers* **24**, 348–350 (1995).
9. H. Nakao, A. Shirakawa, K.-I. Ueda, H. Yagi, and T. Yanagitani, "CW and mode-locked operation of Yb³⁺-doped Lu₃Al₅O₁₂ ceramic laser," *Opt. Express* **20**, 15385–15391 (2012).
10. C.W. Xu, D.W. Luo, J. Zhang, H. Yang, X.P. Qin, W.D. Tan, and D.Y. Tang, "Diode pumped highly efficient Lu₃Al₅O₁₂ ceramic laser," *Laser Phys. Lett.* **9**, 30–34 (2012).
11. A. Toncelli, M. Alshourbagy, and M. Tonelli, "Optical properties of Yb³⁺ doped Lu₃Al₅O₁₂ crystal fibers grown by μ -pulling down technique," *J. Appl. Phys.* **104**, 104916 (2008).
12. J. Tümmler, R. Jung, H. Stiel, P.V. Nickles, and W. Sandner, "High-repetition-rate chirped-pulse-amplification thin-disk laser system with joule-level pulse energy," *Opt. Lett.* **34**, 1378–1380 (2009).

13. I.B. Mukhin, A. Vyatkin, E. Perevezentsev, O. Vadimova, O. Palashov, and E. Khazanov, "Sub-joule level high repetition rate cryogenic disk laser," in CLEO:2011 - Laser Applications to Photonic Applications, OSA Technical Digest (CD) (Optical Society of America, 2011), paper CWP6.
14. F.J. Furch, B.A. Reagan, B.M. Luther, A.H. Curtis, S.P. Meehan, and J.J. Rocca, "Demonstration of an all-diode-pumped soft x-ray laser," *Opt. Lett.* **34**, 3352–3354 (2009).
15. D. Albach, M. Arzakantsyan, G. Bourdet, J.-C. Chanteloup, P. Hollander, and B. Vincent, "Current status of the LUCIA laser system," *J. Phys.* **244**, 032015 (2010).
16. M. Siebold, J. Hein, C. Wandt, S. Klingebiel, F. Krausz, and S. Karsch, "High-energy, diode-pumped, nanosecond Yb:YAG MOPA system," *Opt. Express* **16**, 3674–3679 (2008).
17. M. Siebold, M. Loeser, U. Schramm, J. Koerner, M. Wolf, M. Hellwing, J. Hein, and K. Ertel, "High-efficiency, room-temperature nanosecond Yb:YAG laser," *Opt. Express* **17**, 19887–19893 (2009).
18. S. Banerjee, K. Ertel, P.D. Mason, P.J. Phillips, M. Siebold, M. Loeser, C. Hernandez-Gomez, and J.C. Collier, "High Efficiency 10 J diode pumped cryogenic gas cooled Yb:YAG multi-slab amplifier," *Opt. Lett.* **37**, 2175–2177 (2012).
19. M. Loeser, M. Siebold, F. Roeser, and U. Schramm, "High energy CPA-free picosecond Yb:YAG amplifier," in Lasers, Sources, and Related Photonic Devices, OSA Technical Digest (CD) (Optical Society of America, 2012), paper AM4A.16.
20. C. Stewen, K. Contag, M. Larionov, A. Giesen, and H. Hügel, "A 1-kW CW Thin Disc Laser," *IEEE J. Quantum Electron.* (ST) **6**, 650–657 (2000).

1. Introduction

High-average power, short and ultra-short pulse, diode-pumped solid-state lasers (DPSSLs) have become attractive and powerful tools for laser material processing, laser plasma physics, spectroscopy, remote sensing, and pumping parametric amplifiers [1]. Thin-disk lasers [2] are well suited to generate both high-pulse energies and high-repetition rates due to the possibility of large apertures and low geometrical thickness, which is critical for efficient thermal management. Scaling the output pulse energy of a single thin-disk based laser amplifier head is mainly limited by amplified spontaneous emission (ASE) or even parasitic lasing [3]. However, stacking multiple thin disks [4] or using thicker disks [5] allows generation of pulse energies up to several joules.

Ytterbium-doped materials are attractive for use in DPSSLs because of their low quantum defect and comparably long fluorescence lifetimes. Both the spectroscopic and the thermal properties of the laser host medium are important for the design of a high average and peak power laser. Yb:YAG is one of the most well developed thin-disk laser materials. Recently, Yb:LuAG [6, 7] was investigated as a promising candidate for kW thin-disk lasers because of its superior thermal conductivity compared to Yb:YAG. Along with the high thermal conductivity ($7.4 \text{ W m}^{-1} \text{ K}^{-1}$ for Yb:LuAG and $6.1 \text{ W m}^{-1} \text{ K}^{-1}$ for Yb:YAG at 10% Yb^{3+} -concentration [6]) which is nearly independent from the doping level Yb:LuAG also exhibits reduced reabsorption loss at the laser wavelength which is evident by having a lower minimum excitation level $\beta_{\min} = 5.3\%$, compared to $\beta_{\min} = 5.5\%$ in Yb:YAG. Thus making Yb:LuAG a suitable material for efficient operation of a high energy DPSSL or amplifier at room temperature. Although, first cw-lasing [8], mode-locked fs-operation [9], highly efficient cw-lasing of a ceramic bulk medium [10] and crystal fibers [11] have already been demonstrated, high-energy short-pulse amplification in Yb:LuAG has not been reported so far.

In this paper we demonstrate high-energy ns-pulse amplification in Yb:LuAG and Yb:YAG, as well as a cavity dumped thin-disk laser oscillator based on both materials. We achieve an optical-to-optical efficiency of more than 20%, mainly due to regenerative pumping, which is comparably high for a pulsed laser system operating at room temperature. Previous works reporting on diode-pumped Yb:YAG amplifiers with similar pulse energies [12, 13] or even more than 1 J [14, 15] either demonstrated a maximum optical-to-optical efficiency around 10% or relied on cryogenic cooling, and/or based on bulk material [16–18]. While cryogenically cooled lasers allow for even higher efficiencies the gain spectrum is narrowed dramatically for both

Yb:YAG and Yb:LuAG. Pulses as short as 2 ps, corresponding to a gain bandwidth of about 1 nm, can be amplified at room temperature, whereas at liquid nitrogen temperature the gain bandwidth reduces by about one order of magnitude. Hence, we also studied the spectral response of both materials at room temperature. Although the peak absorption cross section of Yb:LuAG around 940 nm is lower compared to Yb:YAG the broader absorption spectrum is more suitable for using pump diodes without wavelength stabilization. Common high peak-power laser diode stacks for quasi-cw pumping show an integral spectral width between 3 and 10 nm, mainly due to wavelength shift (0.3–0.4 nm/K) over the pump pulse. Thus, in the following experiments we used laser diodes having a spectral width of about 5 nm which leads to equal absorption lengths at the same doping level.

2. Experimental setup

Figure 1 shows the experimental setup of a diode-pumped master oscillator power amplifier (MOPA) using either Yb:LuAG or Yb:YAG as the gain medium. Pulses with a duration of 6 ns at a center wavelength of 1030 nm were generated in a cavity dumped oscillator (see Fig. 1a). For Q-switching the resonator cavity we employed a thin-film polarizer and a KD*P-Pockels cell. A 9 W fiber-coupled laser diode (Lumics GmbH) with a fiber core diameter of 105 μm and a NA of 0.15 was used for pumping at 940 nm. The pump light was collimated and refocused into the gain medium by two spherical lenses, while pump and laser beams were separated by a dichroic mirror.

A concave mirror (radius of curvature: 500 mm) was utilized to form a 800 mm long stable cavity with a mode-size diameter of 200 μm . In a second stage (booster) the ns-pulses were then amplified to about 50 mJ in an Yb:YAG 14-pass amplifier which is similar to the final amplifier in terms of the optical setup (detailed description given in [19]).

The gain medium of the final multi-pass amplifier was pumped by a stack of 25 fast axis collimated diode-laser bars (Jenoptik Lasertechnik GmbH) with a peak output power of 4 kW and a center wavelength of 940 nm. The near field beam profile was imaged onto a single micro-lens array (SÜSS MicroTec AG) for homogenization. In this non-imaging homogenization scheme a spherical lens was used for beam focussing under an angle of 30 degrees. However, we operated close to the Fourier plane in order to achieve a balance between a smooth symmetric pump profile and pump intensity. The reflected pump light was recovered by a 4- f imaging configuration comprising of two lenses and a plane mirror leading to two double-passes of the pump light through the amplifier disk. The resulting pump beam profile (19.2 kW cm⁻² peak intensity at 4 kW pump power) is shown in Fig. 2(a).

Figure 2(b) illustrates the beam profile of the booster output at 50 mJ and a repetition rate of 10 Hz. All stages are optically isolated from each other with a Faraday isolator in order to suppress back-seeding of ASE into the oscillator. The output beam of the booster is magnified to 2.3 mm at full width half maximum (FWHM) by a spherical lens telescope before it is sent into the semi-stable resonator cavity of the final amplifier (see Fig. 1 (b)). A horizontal tilt of the active mirror (Yb:LuAG or Yb:YAG disk) along the vertical axis allowed ten-pass amplification of the seed-pulses within this relay imaging cavity. Here, the incoming and the outgoing beams were vertically separated at M1. No vacuum was required at the focal region between M2 and M3 in order to prevent air breakdown. For astigmatism compensation the collimated beams are reflected under both horizontal and vertical tilt of M2 and M3, respectively. The resulting output beam profile without gain is shown in Fig. 2(c), which also provides an estimation of the aberrations due to optical misalignment.

In the experiments described here we used a ceramic Yb:LuAG disk (produced by Konoshima Chemical Co., Ltd.) with a diameter of 18 mm, a thickness of 1 mm, and an Yb³⁺-concentration of 10.2%. Furthermore, single crystalline Yb:YAG disks with an optical thickness (Yb³⁺-

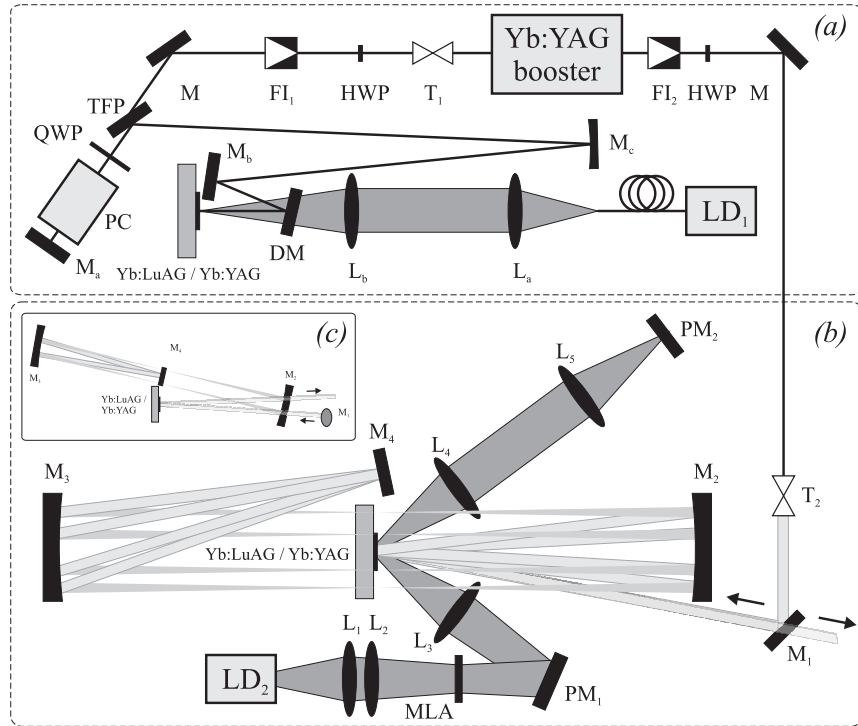


Fig. 1. Experimental setup. (a) ns-oscillator operating in cavity-dumped mode with subsequent Yb:YAG booster: LD1 9 W fiber-coupled laser diode; La, Lb, spherical lenses ($f_a = 50$ mm, $f_b = 100$ mm); DM, dichroic mirror (AR 0° 930–950 nm, HR 0° 1010–1070 nm); Ma, Mb, dielectric flat mirror (HR 0° 1010–1060 nm); Mc, dielectric concave mirror (HR 0° 1010–1060 nm), radius of curvature: 500 mm; TFP thin film polarizer (angle of incidence: 55°); FI1, FI2, Faraday isolator (rotator and polarizers); HWP/QWP, half/quarter wave-plate; PC, KD*P Pockels-cell; T1, T2, spherical lens telescopes; (b) Multipass amplifier (top view): LD2, 4 kW Laser diode stack M, M1, dielectric flat turning mirrors (HR 45° 1010–1060 nm), diameter: 25 mm; M2, M3, dielectric concave mirrors (HR 0° 1010–1060 nm), radius of curvature: 750 mm, diameter: 50 mm; M4, dielectric flat mirror (HR 0° 1010–1060 nm), diameter: 25 mm; L1, toric lens (fast axis: $f_{FA} = 800$ mm; slow axis: $f_{SA} = 115$ mm); L2, spherical lens ($f = 500$ mm); L3, spherical lenses ($f = 100$ mm); L4, L5, spherical lenses ($f = 75$ mm); PM1, PM2 broadband dielectric flat mirror (HR 0° 750–1100 nm); MLA, (AR 750–1100 nm coated) micro-lens array ($f = 10$ mm, size: 15×15 mm², pitch: 500 μ m); (c) side-view of the multi-pass amplifier.

concentration \times thickness) of $2\% \times 2.5$ mm and $5\% \times 3$ mm (produced by Laserayin Tecnica) as well as $3\% \times 3$ mm and $10\% \times 1$ mm (produced by FEE) were employed for comparison. While the $10\% \text{ Yb}^{3+}$ -doped sample had an aperture of 12.5 mm the other Yb:YAG samples were 25 mm in diameter. The gain media of each laser were coated using ion-assisted deposition (IAD) sputtering for high reflectivity (HR) on the back side and for anti-reflection (AR) on the front side (provided by Laseroptik GmbH). Finally, the laser disk was glued on a polished copper plate which was mounted on a water-cooled heat sink. Figure 3 illustrates the optical quality of these compounds investigated by polarimetry and interferometry at a wavelength of 1030 nm. Distortions of the transmitted wavefront are caused by surface deformations due to coating and/or mounting stress. The intrinsic stress birefringence (only in the case of the $5\% \times 3$ mm Yb:YAG disk) is mainly owed to crystal growths striations. Regarding to the

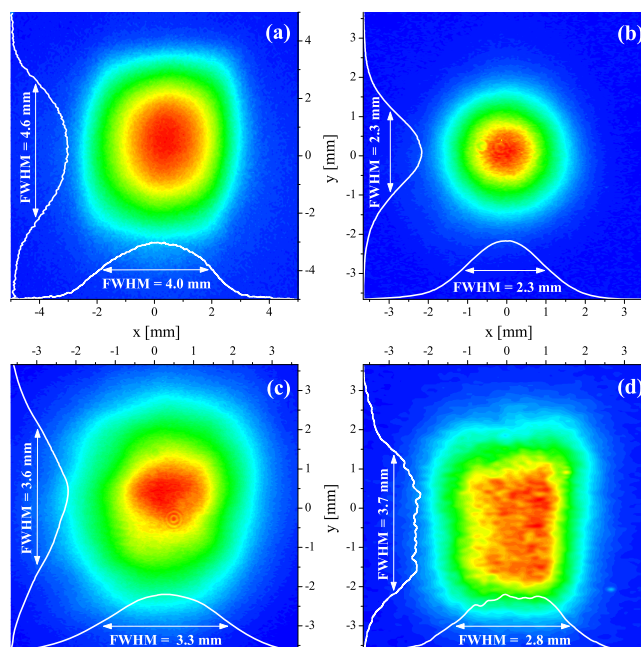


Fig. 2. Beam profiles of the final amplifier: (a) pump profile, (b) seed beam profile, (c) transmitted output beam without gain, (d) amplified output beam.

optical homogeneity of the Yb:LuAG sample no distortions were observed with polarimetry and shadowgraphy.

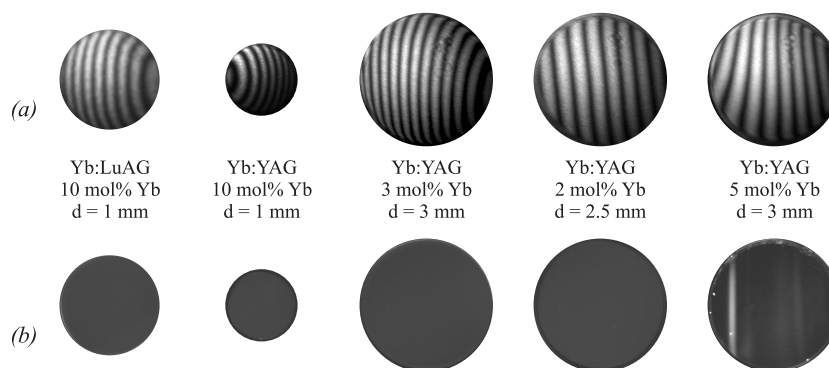


Fig. 3. Optical quality: (a) interferogram and (b) polarogram of the ceramic Yb:LuAG and the crystalline Yb:YAG disks.

3. Experimental results

We first analyzed the behavior of the 1 mm thick Yb:YAG and Yb:LuAG disks with nearly the same optical thickness in the ns-oscillator. Figure 4 compares the performance of the both-configurations. It can be clearly seen that the threshold is reduced in case of Yb:LuAG, due to

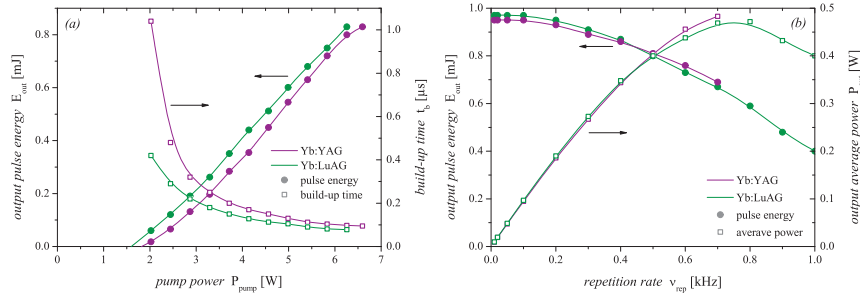


Fig. 4. Dynamic of the cavity-dumped ns-oscillator: (a) Output pulse energy and build-up time vs. pump peak power, pulsed pumping with pump duration of 1 ms and a repetition rate of 10 Hz; (b) Output pulse energy and average output power vs. repetition rate, continuous-wave pumping, pump power: 6.7 W.

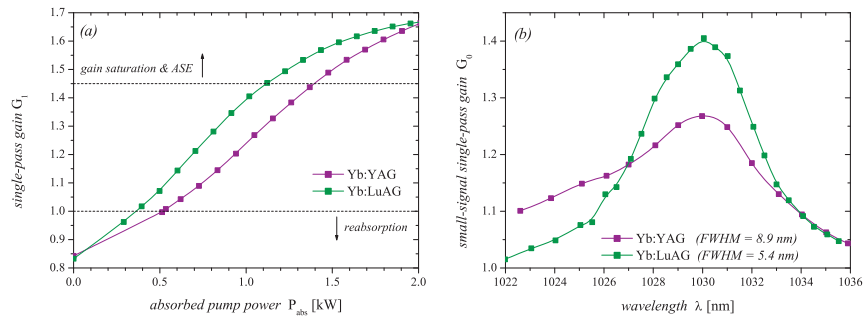


Fig. 5. Single-pass gain of diode-pumped Yb:LuAG and Yb:YAG at a pump pulse duration of 1 ms: (a) single-pass gain calculated from the total gain of a ten-pass amplifier, seed energy: 1 mJ at a wavelength of 1030 nm, (b) tuning range of the small-signal single-pass gain.

the lower β_{min} value. Furthermore, the build-up time required in order to saturate the gain is much lower for Yb:LuAG due to its higher emission cross section at the laser wavelength. To compare performance at high-average powers we also measured the dependence of output power on pulse repetition rate (see Fig. 4(b)). Although the pulse energy in the case of Yb:LuAG is higher than Yb:YAG at low repetition rates a stronger increase of the average output power was observed in Yb:YAG. This is attributable to the longer fluorescence lifetime of Yb:LuAG since the repetition rate for maximum output power is dependent on the inverse of the fluorescence lifetime.

In the next step we investigated the small-signal gain of both materials in a multi-pass amplifier, configured for ten passes (see Fig. 1(b)). Because of the higher emission cross section and lower β_{min} -value of Yb:LuAG the pump energy required to bleach out reabsorption is lower and the single-pass gain higher with respect to the absorbed pump power than Yb:YAG (see Fig. 5(a)). In order to determine the spectral behavior of the gain media corresponding to the gain cross section we measured the small-signal gain with a tunable seed source (bandwidth: 0.2 nm, tunable between 1022 and 1036 nm, pulse duration: 6 ns). To prevent gain saturation in the Yb:YAG and Yb:LuAG disks we limited absorbed pump peak power (calculated from pump light transmission) to 1.1 kW at a pump duration of 1 ms, corresponding to a pump fluence of 5.3 J cm^{-2} . The result is summarized in Fig. 5(b). It is clear that the higher gain of Yb:LuAG compared to Yb:YAG is accompanied by a narrower tuning range and gain bandwidth.

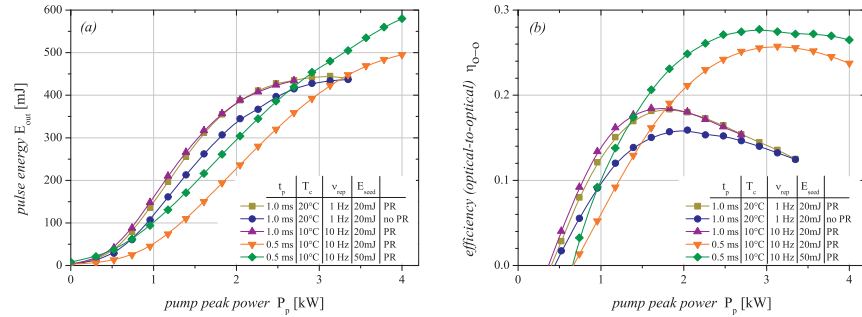


Fig. 6. Dynamic of the Yb:LuAG Multi-pass amplifier: (a) Output pulse energy and (b) optical-to-optical conversion efficiency vs. pump peak power: t_p , pump duration; T_c , cooling water temperature; v_{rep} , repetition rate; PR, pump recovery (i.e. 4 pump passes).

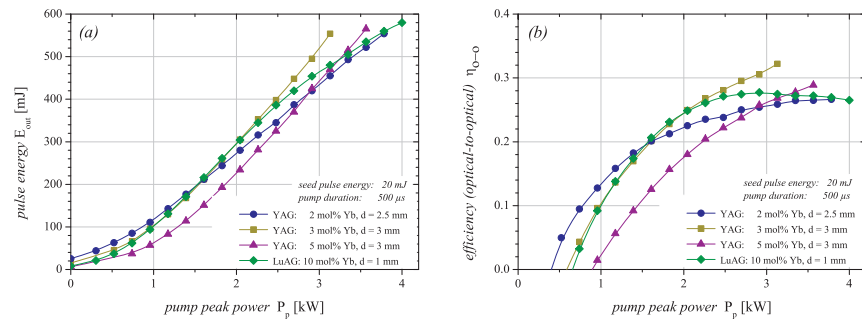


Fig. 7. Comparison of the multi-pass amplifier output between Yb:LuAG and Yb:YAG with different doping and thickness: (a) Output pulse energy and (b) optical-to-optical conversion efficiency vs. pump peak power.

Demonstration of efficient high energy operation was performed in the final multi-pass amplifier where gain saturation was achieved by seeding with a high pulse energy (i.e. $\approx 10\%$ of the desired output energy). The performance of the multi-pass amplifier with Yb:LuAG as the gain medium is given in Fig. 6. We obtained an optical-to-optical conversion efficiency of 28% for a pump pulse duration of 0.5 ms, seed pulse energy of 50 mJ and a pump peak power of 2.8 kW. The drop in efficiency observed at higher pump intensities can be explained by excessive amounts of ASE inside the gain medium, due to the high aspect ratio between pump spot diameter and disk thickness (see [3]). This effect becomes more obvious at longer pump pulses (e.g. 1 ms), where the amount of stored energy at which ASE occurs is reached at a lower pump power.

In Fig. 7 we show the performance of the same amplifier using Yb:YAG with different dimensions and doping. Unfortunately, the 1 mm Yb:YAG disk could not be used for a direct comparison with the Yb:LuAG sample because the wavefront deformations over the full aperture (see Fig. 3) could not be compensated. However, the Yb:YAG sample with the same optical thickness (3%, $d = 3$ mm) as the Yb:LuAG disk used in the previous experiments performs similarly at low pump powers, while no drop of efficiency due to ASE was detected at higher pump intensities. It has to be mentioned that the design of the amplifier disk in terms of the thickness and doping level has a strong impact on the extraction efficiency, which can be seen from the experiments done solely with Yb:YAG. While at low pump intensities a low optical thickness leads to lower reabsorption loss (lower threshold fluence), the losses due to unabsorbed pump

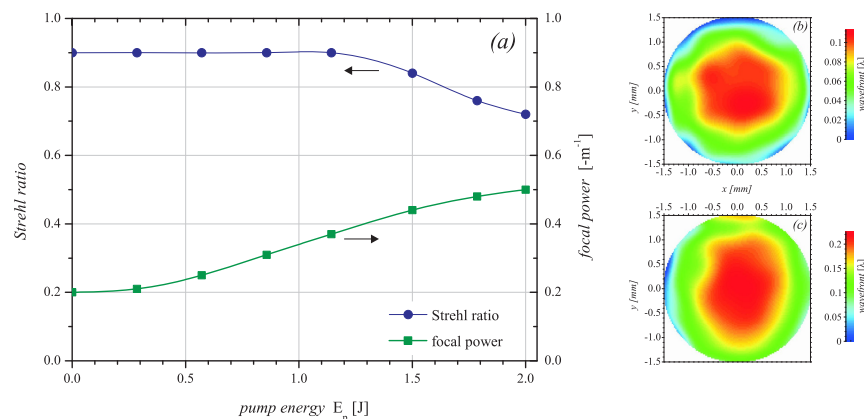


Fig. 8. Wavefront analysis of the amplified output pulses: (a) Strehl ratio and focal power (divergent beam) vs. pump energy at a repetition rate of 10 Hz, (b) wavefront at 0.6 J, and (c) wavefront at 2 J pump energy, (wavelength $\lambda = 1030$ nm).

light increase with higher pump intensities. In general, it can be stated that a higher gain and lower reabsorption such as in case of Yb:LuAG improve the optical-to-optical conversion efficiency.

In the case of the 3%-doped Yb:YAG sample we achieved 560 mJ output for a pump peak power of 3.2 kW and 0.5 ms pulse duration at a repetition rate of 1 Hz, corresponding to an optical-to-optical conversion efficiency of 32%. Only in case of the 2% Yb³⁺-doped Yb:YAG and the Yb:LuAG disk were we able to operate at 10 Hz repetition rate. When changing the repetition rate from 1 to 10 Hz and reducing the heat sink temperature by 10 K, we observed nearly the same output versus pump energy (see Fig. 6). The repetition rate for all the more highly-doped Yb:YAG samples was limited by the onset of thermal instabilities and/or material damage due to their increased thickness and the reduction in thermal conductivity for doping levels >2% Yb³⁺.

During the experiments (approx. 1 minute per data point) we observed energy fluctuations of $\approx 2\%$ (peak to valley), whereas the oscillator instabilities (i.e. $\approx 5\%$) were damped due to gain saturation of the subsequent amplifiers. Figure 2(d) shows the output beam spatial profile of the Yb:LuAG multipass amplifier at full energy. It is evident that the shape of the output beam converges to that of the pump beam profile due to gain saturation in the center of the beam. Slight spatial gain narrowing was observed, especially during the first amplifier passes, when the gain was not fully saturated. Finally, the wavefront of the amplifier output pulses was recorded with a Shack-Hartmann sensor (Optocraft SHSLab HR-150-GE). Figure 8 illustrates the evolution of the Strehl ratio and the beam divergence. The beam quality and the focal power depend on both, the amplifier alignment and the wavefront transmission through the gain medium. Additional aberrations due to thermally induced bending or bulging [20] of the amplifier disk were observed at higher pump energies. In this case the deformation of the disk overcompensates the (positive) thermal lens which arises from the temperature gradient and the refractive index change dn/dT .

4. Conclusion

In this paper, we have presented nanosecond pulse generation in a cavity-dumped oscillator and compared the performance of Yb:LuAG and Yb:YAG as thin-disk laser materials. With regard to their spectroscopic properties we found a profound improvement of the small-signal gain and

reduced lasing threshold when employing Yb:LuAG instead of the standard Yb:YAG. In terms of broadband pulse amplification we obtained a tuning range of 8.9 nm in the case of Yb:YAG and 5.4 nm for Yb:LuAG. At narrow bandwidth operation however, Yb:LuAG shows better lasing performance especially at high average powers due to its improved thermal properties. We obtained ns-pulse amplification in a ceramic Yb:LuAG disk up to an energy of 550 mJ at an optical-to-optical conversion efficiency of 28%, while at the maximum energy of 580 mJ the efficiency dropped to 26% due to ASE. Although higher efficiency operation was limited by parasitic lasing we achieved to the best of our knowledge the highest optical-to-optical conversion efficiency for room temperature nanosecond diode-pumped Ytterbium based lasers at this energy level. Regarding to the optical quality required in high-energy laser amplifiers ceramic Yb:LuAG (and Yb:YAG) favorably competes with single crystalline material especially at large apertures.

A discrete number of disk parameters have been studied in order to assess the viability of the thin-disk or active mirror concept for use in high energy short pulse amplifiers. This study has confirmed that further scaling of both efficiency and pulse energy is possible by a further reduction of Yb-doping level reducing the gain per disk. This, however, requires additional passes for pump recovery as well as multiple disks in order to obtain a similar gain per amplifier stage. In summary, on the basis of the experiments presented here we believe Yb:LuAG is a promising candidate for applications in high energy, diode-pumped laser amplifiers.